A Flexible Glass Fiber Based Freestanding Composite Electrode for High-Performance Lithium Polysulfide Batteries

P. Ragupathy,* Syed Abdul Ahad, P. Ramesh Kumar, Hyun-Wook Lee, and Do Kyung Kim*

Herein, a flexible, low-cost, and freestanding membrane electrode (FSME) in lithium polysulfide batteries with high energy density and long cycle life is reported. The specially designed electrode offers adequate space to accommodate a large amount of sulfur and facilitate the enhanced immobilization of polysulfide ions. Moreover, polar-based oxides inbuilt in the electrode favor in suppressing the polysulfide shuttling effect. The initial specific capacity of Li polysulfide (Li_2S_8) in FSME is 1210 mAh g^{-1} at 0.2 C with remarkable capacity retention upon cycling. The capacity stabilizes at 970 mAh g^{-1} at 100th cycle indicating the excellent cycling ability of FSME. Further, this membrane electrode alleviates the cost issues associated with most of the carbon nanotube-based electrodes.

The development of high-performance rechargeable batteries has recently attracted great interest due to the huge requirement of energy storage for personal electronic devices, electric vehicles, and large-scale storage of electricity.[1–7] In this regard, lithium–sulfur (Li–S) battery has been widely recognized as one of the major rechargeable energy storage systems due to its high theoretical specific capacity of 1675 mAh g^{-1} and high theoretical specific energy density of 2600 Wh kg^{-1}.[8–11] Moreover, sulfur is known as an earth-abundant material available at large scale, making it very attractive for a low cost and high energy density Li–S batteries.[3,8,9] Despite the several considerable merits of Li–S, the commercialization of Li–S technology has not been fully realized due to the low electrical conductivity of sulfur (5×10^{-30} S cm^{-1} at 25 °C), high solubility and diffusivity of polysulfides intermediates, volume expansion, and the related side reaction caused by the shuttle effect.[3,10–13]

Prof. P. Ragupathy, S. A. Ahad, Dr. P. R. Kumar, Prof. D. K. Kim
Department of Materials Science and Engineering
Korea Advanced Institute of Science and Technology (KAIST)
Daejeon 305-701, Republic of Korea
E-mail: ragupathyp@cecri.res.in; dkkim@kaist.ac.kr
Prof. P. Ragupathy
Electrochemical Power Sources Division
Fuel Cells Section, Central Electrochemical Research Institute
Karaikudi 630 003, India
S. A. Ahad, Prof. H.-W. Lee
School for Energy and Chemical Engineering
Ulsan National Institute of Science and Technology (UNIST)
Ulsan 44919, Republic of Korea

The ORCID identification number(s) for the author(s) of this article can be found under https://doi.org/10.1002/adsu.201700083.

In order to address these issues, all kinds of carbon–sulfur (C–S) composites such as mesoporous C–S composites, active carbon–S composites, carbon nanotubes (CNT)–S composites, hollow carbon nanofibers–S composites, and graphene–S composites have been proposed as active materials in cathodes to achieve significant cycling performance.[14–23] A new architecture design to buffer the volumetric expansion/shrinkage[7,24] and modifying the electrode to confine the lithium polysulfides suppressing the shuttling effects[25–28] are also explored. Moreover, many attempts have been made to encapsulate the polysulfide within the cathode by establishing advanced cathode architectures.[29–31] However, all these exciting studies reveal that there is still significant amount of polysulfide dissolution in the electrolyte after cycling of the cells.[32,33]

Conventionally, the electrode fabrication process involves the use of auxiliary components materials, such as conductive carbon, binder, and metallic current collectors offsetting the high energy density of Li–S batteries. Easy delamination of active materials and lithium diffusion kinetics are main challenges in the flat current collectors. Recently, well-engineered 3D battery design has been popularized as an alternate to improve the overall energy density and areal capacity. For instance, Li et al. have reported 3-dimensional (3D) porous carbon composites[34] containing a large amount of sulfur nanoparticles exhibiting a high sulfur utilization with a high specific capacity and a long cycling life. A flexible 3D graphene foams and framework to accommodate a large amount of sulfur with high areal capacity and to increase the sulfur areal mass loading in the composite electrodes, respectively.[13,35] However, with these strategies, the internal sulfur within the electrode is not fully utilized due to limited access of an electrolyte, which leads to phenomenon of "sulfur activation."[13,35,36]

Use of lithium polysulfides as active materials has several merits over the solid sulfur as the precursor followed by melt-diffusion or liquid infiltration routes. It is proven that lithium polysulfides improve sulfur utilization minimizing the effect of sulfur activation. Moreover, lithium polysulfide (LPS) alleviate any structural changes within an electrode and facilitates the kinetics of the Li–S redox reactions impacting on the rate capability.[9,10,37,38] There are earlier reports on lithium polysulfides systems with various materials including carbon nanotubes, carbon nanofibers, and graphene and N, S-co-doped

**ADVANCED
SCIENCE NEWS**

www.advancedsciencenews.com

**ADVANCED
SUSTAINABLE
SYSTEMS**

www.advsustainsys.com

graphene.[13,39–42] However, all these exciting works are based on CNT as electrode materials in which cost is one of the main obstacles for its commercialization.

Inspired by the low cost and environmentally benign nature of glass fiber membrane, we present here a flexible and a free-standing electrode composed of glass fiber membrane, and MnO_2 particles become an adequate host for Li polysulfide batteries. The glass fiber membrane acts as a decent reservoir for liquid polysulfide, while a small amount of multiwalled CNT (MWCNT) provides a large conductive network throughout the matrix. More importantly, MnO_2 particles decorated on GF can make strong bonds with LPS reducing the shuttle effect. To the best of our knowledge, there is no report on the utilization of glass membrane electrode for Li–S batteries. The remarkable cycling ability and high reversibility are caused by the combination of a decent reservoir for polysulfides, chemical binding of LPS, and balanced conductivity due to glass fiber membrane, MnO_2 particles, and MWCNT, respectively, making this flexible membrane best electrode materials for Li–S batteries.

The flexible freestanding GF/MWMCNT/MnO_2 host electrode for Li polysulfide was fabricated using a vacuum filtration technique. The self-weaving nature of different types of commercial carbon nanotubes (single-walled, double-walled, and multiwalled) is frequently noticed and this fabrication method has been adopted to prepare CNT electrodes for Li-ion batteries.[43] A similar self-weaving technique is extended to glass fibers (Whatman glass fibers) to fabricate the flexible electrodes for the first time. In the GF/MWCNT/MnO_2 freestanding electrodes, the LPS liquid can easily penetrate and uniformly distribute on glass fibers, MnO_2, and MWCNT. Formation of MnO_2 in the presence of butyric acids was reported previously by our group.[44] As presented in **Figure 1**, MWCNTs would facilitate the fast electronic conductivity, while MnO_2, due to its polar nature, provides strong chemical binding toward polysulfides. In addition to MWCNTs and MnO_2, the glass fibers operated as a reservoir to absorb polysulfide in the GF/MWCNT/MnO_2 electrode. Moreover, $LiNO_3$ was added in the

electrolyte as an addictive to form a uniform passive layer on the lithium foil preventing lithium corrosion and electrolyte loss.[45]

To confirm the crystal structure and phase purity of the synthesized materials, X-ray diffraction (XRD) analysis was carried out. Accordingly, Figure S1 (Supporting Information) shows the powder XRD patterns of pristine glass fibers, MWCNT, as prepared in MnO_2 and GF/MWCNT/MnO_2. The poor crystalline nature of the as-synthesized MnO_2 is revealed by the presence of a broad peak of around 2θ value of 37°. The formation of δ-MnO_2 is indicated by the presence of the amorphous XRD pattern which is well studied.[44,46] The sharp peak at $2\theta = 26.38°$ and the small broad peak at $2\theta = 43.38°$ are observed as corresponding, respectively, to the (002) plane and (100) plane of graphitized MWCNTs.[47] A broad peak at $2\theta = 26°$ of membrane indicates the amorphous nature of the fiber. Accordingly, the XRD pattern of GF/MWCNT/MnO_2 composite shows the characteristic nature of all the components present in its matrix.

Morphological changes were investigated using a scanning electron microscope (SEM) and a transmission electron microscope (TEM) with elemental mapping of the GF/MWCNT/MnO_2 electrodes. Accordingly, the SEM image (**Figure 2**a) shows that the GF and MWCNT are well enlaced forming a mired network, which facilitates efficient ion diffusion/mass transfer, and also provides enough interspatial region to accommodate a large amount of polysulfides. Glass fiber exhibits a smooth surface with a diameter of ≈0.5–1 μm, and several micrometers in length. Such hierarchical network can be regarded as the buffering/absorption reservoir of polysulfides.[48] Figure 2b shows the TEM images of GF/MWCNT/MnO_2 indicating a clear well-wrapped MWCNT over the fibers. Both fibers and MWCNTs possess well-defined 1D structures in which MWCNTs is 15 nm in diameter and a few micrometers in length. Many MnO_2 particles are attached to the surface of nanotubes as well as on the glass fiber as marked (yellow circles) in Figure 2c. Unlike other 2D graphene materials, such 3D interconnected networks can offer multidimensional electron transport pathways due to the easy accessibility of the electrolyte into GF/MWCNT/MnO_2. The cross-sectional SEM image of GF/MWCNT/MnO_2 is shown in Figure S2 (Supporting Information) indicating the highly porous intertwined glass fiber and MWCNT for maximum polysulfide absorption. The approximate thickness of the GF/MWCNT/MnO_2 electrode is 134 μm, thus again indicating the presence of a large reservoir for accommodating polysulfides and precipitated sulfur during cycling. Scanning transmission electron microscope (STEM) characterization was used to understand the elements distributed over the fiber matrix. Accordingly, Figure 2d displays STEM image and the corresponding elemental mapping results revealing the homogenous dispersion of C, O, Si, and Mn. As expected, Si and O take up a large proportion of the glass fibers, while C and Mn are found to be evenly distributed all over the composite, as shown in the STEM image. This further reaffirms the notion that all three components are uniformly mixed and MnO_2 is precipitated on glass fibers and MWCNTs using the synthesis procedure adopted. Figure 2d is the pictorial evidence of the flexible electrodes. These films were then punched into electrodes of $\Phi = 12$ mm (Figure S3, Supporting Information) for assembling coin cells.
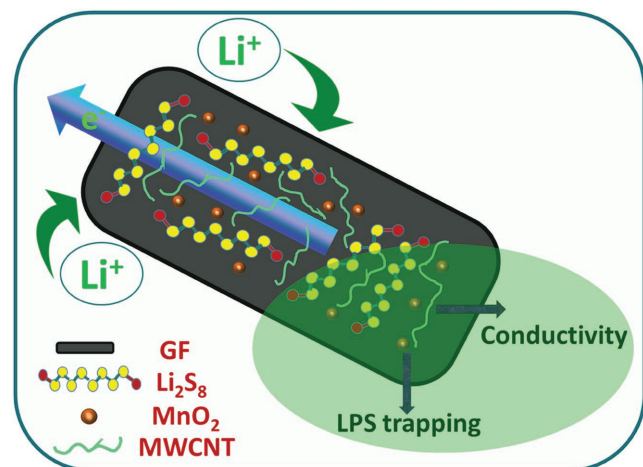

Figure 1. A concept illustration of flexible freestanding GF/MWCNT/MnO_2 electrode with further elaboration of the role of each component in the electrode.
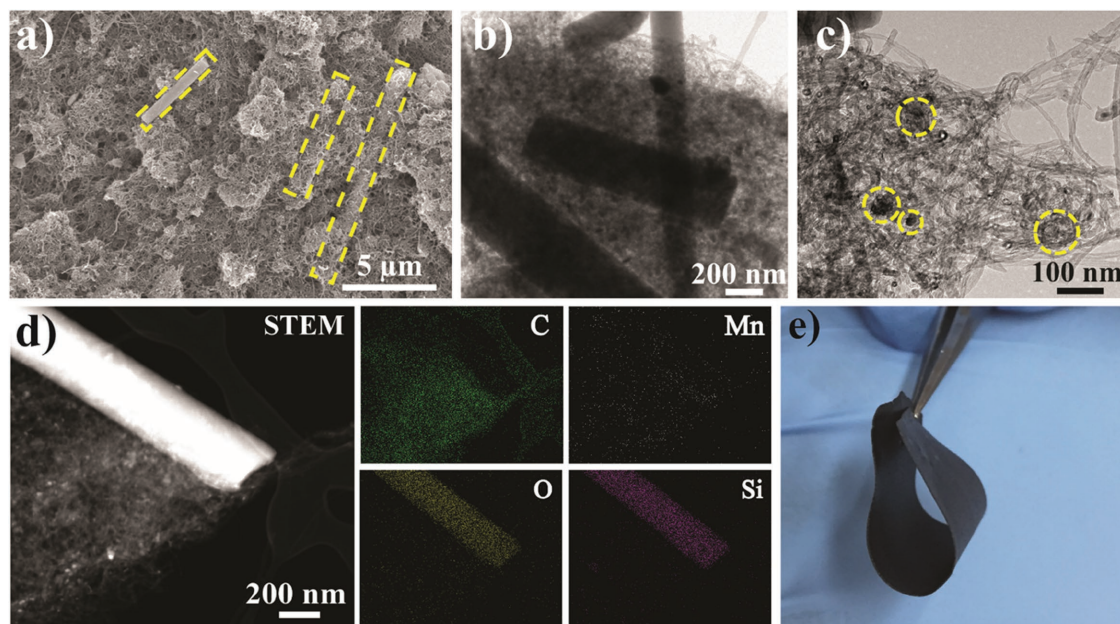
ADVANCED
SCIENCE NEWS
www.advancedsciencenews.com

ADVANCED
SUSTAINABLE
SYSTEMS
www.advsustainsys.com

Figure 2. a) SEM analysis of GF/MWCNT/MnO$_2$ with yellow dotted lines showing glass fibers, b,c) TEM analysis with dotted circles showing MnO$_2$ particles, d) STEM and the corresponding elemental mapping of selected region, and e) as-prepared flexible electrode film of GF/MWCNT/MnO$_2$ composite.

In order to understand the lithium polysulfide interaction with MnO$_2$, an adsorption test was conducted using 2×10^{-3} M Li$_2$S$_8$ solution. The Li$_2$S$_8$ solution was initially dark yellow in color as evident in **Figure 3**a(i). The addition of MnO$_2$ particles in the Li$_2$S$_8$ solution resulted in a concomitant change in color from dark yellow to colorless (Figure 3a(ii)). This strongly suggests that MnO$_2$ exhibits a remarkable polysulfide adsorption ability. The polysulfide interaction with MnO$_2$ particles is clearly reflected in the cycling ability (discussed later). The strong adsorption capability of MnO$_2$ particles with LPSs is mainly attributed to high surface area of MnO$_2$ particles favoring enhanced cycling ability. The UV–Vis spectra of 2×10^{-3} M lithium polysulfide solution with and without MnO$_2$ are shown in Figure 3b. The UV–Vis spectra of bare Li$_2$S$_8$ solution show a broad peak of around 620 nm and also between 400 and 500 nm, which represents the presence of S$_3^{\bullet -}$ as well as higher order polysulfides (S$_8^{2-}$, S$_6^{2-}$, S$_4^{2-}$), respectively.[49]

On the other hand, the characteristic peaks of polysulfide species have completely disappeared upon the incorporation of MnO$_2$ particles, thus, reaffirming the strong chemical binding between polysulfides and our suggested matrix (i.e., GF/MWCNT/MnO$_2$).

With an aim to study the effect of the GF/MWCNT/MnO$_2$ electrode on the electrochemical performance of Li polysulfide batteries; coin cells with lithium metal as the counter/reference electrode were fabricated. Subsequently, the known volume of polysulfide catholyte (0.5 M Li$_2$S$_8$) (5 mg cm^{-2}) was added onto the GF/MWCNT/MnO$_2$ composite electrode. The cells made with GF/MWCNT/MnO$_2$ electrodes were subjected to galvanostatic charge–discharge cycling. Thus, **Figure 4**a depicts the typical charge–discharge profiles of GF/MWCNT/MnO$_2$ composite electrodes at different C-rates (0.1, 0.2, 0.5, and 1 C), indicating the two plateaus during the discharge process that correspond to the two-step reaction mechanism of
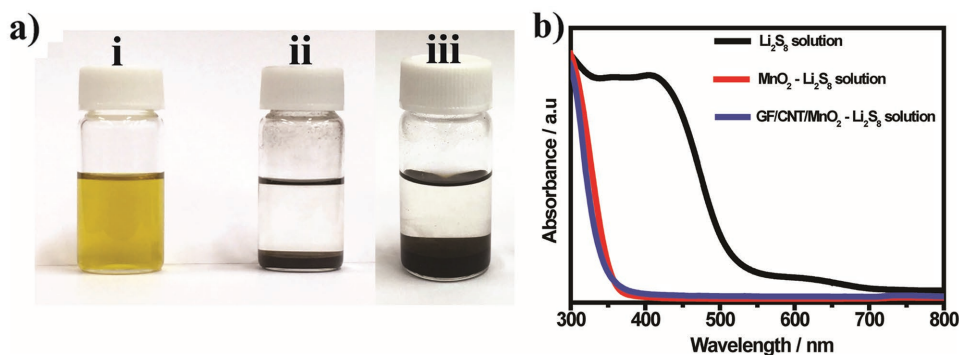

Figure 3. a) Pictorial evidence of the color change of (i) 2×10^{-3} M Li$_2$S$_8$ solution upon addition of (ii) MnO$_2$ nanoparticles and (iii) GF/MWCNT/MnO$_2$. b) Corresponding UV–Vis spectrum of Li$_2$S$_8$ solution before and after addition of MnO$_2$ and GF/MWCNT/MnO$_2$.

**ADVANCED
SCIENCE NEWS**

www.advancedsciencenews.com

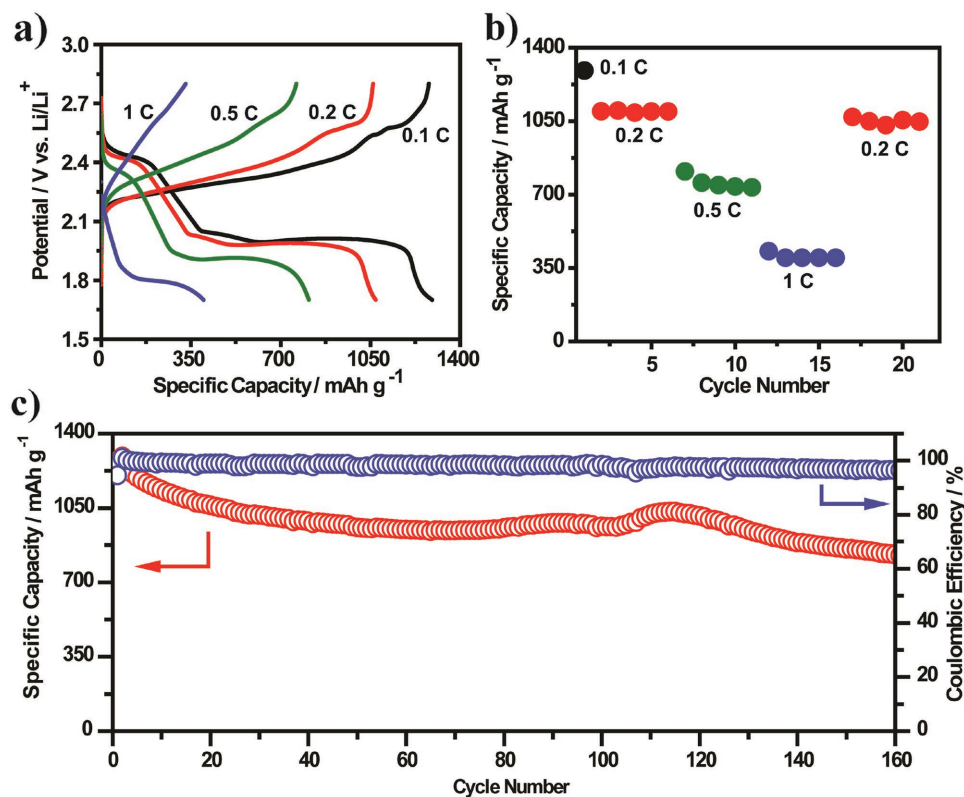**ADVANCED
SUSTAINABLE
SYSTEMS**

www.advsustainsys.com

Figure 4. a,b) Voltage–capacity and corresponding rate capability profile at various C-rates, c) cyclic performance cycled between 2.8 and 1.7 V at 0.2 C with GF/MWCNT/MnO$_2$ used as a cathode film in Li polysulfide battery.

the Li–S battery.[10,50] The two plateaus during discharging are attributed to the solid sulfur and soluble lithium polysulfide (Li$_2$S$_x$, $4 \le x \le 8$) and further reduction to insoluble Li$_2$S$_2$ and Li$_2$S. Correspondingly, while charging again, the two-voltage plateau appeared, confirming the conversion of lithium polysulfides back to elemental sulfur. The corresponding cyclic voltammetry data are shown in Figure S4 (Supporting Information). The initial discharge capacity was found to be 1270 mAh g^{-1} at 0.1 C. The specific capacity, volume of polysulfide, weight of sulfur and weight of GF/MWCNT/MnO$_2$ electrodes are tabulated in Table S1 (Supporting Information). This enhancement in capacity is mainly attributed to high utilization of active sulfur available in the electrolyte. This value is comparable with most of the CNT-based electrodes. The average discharge capacities of GF/MWCNT/MnO$_2$ electrodes at 0.1, 0.2, 0.5, and 1 C are, respectively, 1270, 1080, 750, and 400 mAh g^{-1}, unveiling significant rate performance of fiber electrodes. A discharge capacity of 1070 mAh g^{-1} at the rate of 0.2 C was retained after a high C-rate of 1 C, thus revealing the significant impact of GF/MWCNT/MnO$_2$ on rate performance.

To understand the feasibility of practical application, a cycle-life test was performed at 0.2 C rate. The cell made with GF/MWCNT/MnO$_2$ composite exhibits the initial discharge capacity of 1210 mAh g^{-1}. Correspondingly, the GF/MWCNT electrode without MnO$_2$ addition exhibits a low initial capacity of 890 mAh g^{-1} with severe capacity decay after just 40 cycles as shown in Figure S5 (Supporting Information). In the

subsequent cycles, the GF/MWCNT/MnO$_2$ electrode delivers 1031 mAh g^{-1} at the 25th cycle, which further stabilizes 970 mAh g^{-1} at the 100th cycle. Moreover, the specific capacity of 824 mAh g^{-1} was retained after 160 cycles indicating the excellent cycling stability of a glass fiber electrode. The cell further delivers a columbic efficiency of ≈99% during the course of cycling at 0.2 C as shown in Figure 4c. This enhanced cycling performance of GF/MWCNT/MnO$_2$ is mainly attributed to (i) accommodation of large amount of active materials which improves the polysulfide utilization owing to 3D integrated network of glass fiber and MWCNT, (ii) buffering volume change of the active material during cycling, and (iii) chemical binding of polar MnO$_2$ with lithium polysulfide reduces the shuttle effect realizing the excellent rate performance in lithium–sulfur batteries.

In summary, we have demonstrated specifically new designed flexible electrodes of glass fibers (GF/MWCNT/MnO$_2$) as a sulfur host for stable Li-polysulfide batteries. In this novel design, GF serves as a reservoir for Li$_2$S$_8$ to enhance the immobilization of polysulfide ions, MWCNT provides a good conductive network to maximize sulfur utilization, while the inbuilt polar MnO$_2$ prevents a shuttle effect through a strong chemical binding between MnO$_2$ and lithium polysulfides. Such an innovative designed architecture of flexible and freestanding electrodes enables the achievement of high capacity and remarkable cycling ability for the high-performance of Li–S batteries. We believe that this work will open a new avenue in the development of high energy density and stable Li–S batteries.

Supporting Information

Acknowledgements

Conflict of Interest

The authors declare no conflict of interest.

Keywords

[1] J. M. Tarascon, M. Armand, *Nature* **2001**, *414*, 359.
[2] B. Dunn, H. Kamath, J.-M. Tarascon, *Science* **2011**, *334*, 928.
[3] S. Evers, L. F. Nazar, *Acc. Chem. Res.* **2013**, *46*, 1135.
[4] Y. Yang, G. Zheng, Y. Cui, *Chem. Soc. Rev.* **2013**, *42*, 3018.
[5] J. Zhang, H. Hu, Z. Li, X. W. Lou, *Angew. Chem., Int. Ed.* **2016**, *55*, 3982.
[6] X. Liang, C. Hart, Q. Pang, A. Garsuch, T. Weiss, L. F. Nazar, *Nat. Commun.* **2015**, *6*, 5682.
[7] W. Zhou, Y. Yu, H. Chen, F. J. Disalvo, H. D. Abruna, *J. Am. Chem. Soc.* **2013**, *135*, 16736.
[8] P. G. Bruce, S. a. Freunberger, L. J. Hardwick, J.-M. Tarascon, *Nat. Mater.* **2012**, *11*, 19.
[9] A. Manthiram, Y. Fu, Y. S. Su, *Acc. Chem. Res.* **2013**, *46*, 1125.
[10] A. Manthiram, Y. Fu, S. H. Chung, C. Zu, Y. S. Su, *Chem. Rev.* **2014**, *114*, 11751.
[11] Z. Liang, G. Zheng, W. Li, Z. W. Seh, H. Yao, K. Yan, D. Kong, Y. Cui, *ACS Nano* **2014**, *8*, 5249.
[12] Y. Yang, G. Zheng, S. Misra, J. Nelson, M. F. Toney, Y. Cui, *J. Am. Chem. Soc.* **2012**, *134*, 15387.
[13] G. Zhou, E. Paek, G. S. Hwang, A. Manthiram, *Nat. Commun.* **2015**, *6*, 7760.
[14] S. Moon, Y. H. Jung, D. K. Kim, *J. Power Sources* **2015**, *294*, 386.
[15] J. Schuster, G. He, B. Mandlmeier, T. Yim, K. T. Lee, T. Bein, L. F. Nazar, *Angew. Chem., Int. Ed.* **2012**, *51*, 3591.
[16] N. Jayaprakash, J. Shen, S. S. Moganty, A. Corona, L. A. Archer, *Angew. Chem., Int. Ed.* **2011**, *50*, 5904.
[17] X. Ji, S. Evers, R. Black, L. F. Nazar, *Nat. Commun.* **2011**, *2*, 325.
[18] C. Wang, W. Wan, J.-T. Chen, H.-H. Zhou, X.-X. Zhang, L.-X. Yuan, Y.-H. Huang, *J. Mater. Chem. A* **2013**, *1*, 1716.
[19] S. Xin, L. Gu, N. H. Zhao, Y. X. Yin, L. J. Zhou, Y. G. Guo, L. J. Wan, *J. Am. Chem. Soc.* **2012**, *134*, 18510.
[20] G. Zhou, D.-W. Wang, F. Li, P.-X. Hou, L. Yin, C. Liu, G. Q. (Max) Lu, I. R. Gentle, H.-M. Cheng, *Energy Environ. Sci.* **2012**, *5*, 8901.
[21] Z. Li, J. Zhang, X. W. Lou, *Angew. Chem., Int. Ed.* **2015**, *54*, 12886.
[22] S. Lu, Y. Cheng, X. Wu, J. Liu, *Nano Lett.* **2013**, *13*, 2485.
[23] W. Zhou, H. Chen, Y. Yu, D. Wang, Z. Cui, F. J. Disalvo, *ACS Nano* **2013**, *7*, 8801.
[24] W. Y. Li, G. Y. Zheng, Y. Yang, Z. W. Seh, N. Liu, Y. Cui, *Proc. Natl. Acad. Sci. USA* **2013**, *110*, 7148.
[25] R. Ponraj, A. G. Kannan, J. H. Ahn, D. W. Kim, *ACS Appl. Mater. Interfaces* **2016**, *8*, 4000.
[26] K.-S. K. Park, J. H. Cho, J. Jang, B. Yu, A. T. D. La Hoz, M. Kevin, C. J. Ellison, J. B. Goodenough, *Energy Environ. Sci.* **2015**, *8*, 2389.
[27] S. H. Chung, A. Manthiram, *Adv. Mater.* **2014**, *26*, 7352.
[28] X. Han, Y. Xu, X. Chen, Y. C. Chen, N. Weadock, J. Wan, H. Zhu, Y. Liu, H. Li, G. Rubloff, C. Wang, L. Hu, *Nano Energy* **2013**, *2*, 1197.
[29] S. Moon, Y. H. Jung, W. K. Jung, D. S. Jung, J. W. Choi, D. K. Kim, *Adv. Mater.* **2013**, *25*, 6547.
[30] Y. S. Su, A. Manthiram, *Nat. Commun.* **2012**, *3*, 1166.
[31] G. He, S. Evers, X. Liang, M. Cuisinier, A. Garsuch, L. F. Nazar, *ACS Nano* **2013**, *7*, 10920.
[32] X. Ji, K. T. Lee, L. F. Nazar, *Nat. Mater.* **2009**, *8*, 500.
[33] Z. W. Seh, W. Li, J. J. Cha, G. Zheng, Y. Yang, M. T. McDowell, P.-C. Hsu, Y. Cui, *Nat. Commun.* **2013**, *4*, 1331.
[34] G. Li, J. Sun, W. Hou, S. Jiang, Y. Huang, J. Geng, *Nat. Commun.* **2016**, *7*, 10601.
[35] S. Lu, Y. Chen, X. Wu, Z. Wang, Y. Li, *Sci. Rep.* **2014**, *4*, 4629.
[36] L. Miao, W. Wang, K. Yuan, Y. Yang, A. Wang, *Chem. Commun.* **2014**, *50*, 13231.
[37] Y. Yang, G. Zheng, Y. Cui, *Energy Environ. Sci.* **2013**, *6*, 1552.
[38] X. Pu, G. Yang, C. Yu, *Adv. Mater.* **2014**, *26*, 7456.
[39] X. Yu, Z. Bi, F. Zhao, A. Manthiram, *ACS Appl. Mater. Interfaces* **2015**, *7*, 16625.
[40] Y.-S. Su, A. Manthiram, *Chem. Commun.* **2012**, *48*, 8817.
[41] Y. Fu, Y. S. Su, A. Manthiram, *Angew. Chem., Int. Ed.* **2013**, *52*, 6930.
[42] S. Moon, J.-K. Yoo, Y. H. Jung, J.-H. Kim, Y. S. Jung, D. K. Kim, *J. Electrochem. Soc.* **2017**, *164*, A6417.
[43] S. Y. Chew, S. H. Ng, J. Wang, P. Novák, F. Krumeich, S. L. Chou, J. Chen, H. K. Liu, *Carbon* **2009**, *47*, 2976.
[44] Y. Munaiah, B. G. S. Raj, T. P. Kumar, P. Ragupathy, *J. Mater. Chem. A* **2013**, *1*, 4300.
[45] H. Yao, G. Zheng, P.-C. Hsu, D. Kong, J. J. Cha, W. Li, Z. W. Seh, M. T. McDowell, K. Yan, Z. Liang, V. K. Narasimhan, Y. Cui, *Nat. Commun.* **2014**, *5*, 3943.
[46] P. Ragupathy, D. H. Park, G. Campet, H. N. Vasan, S. J. Hwang, J. H. Choy, N. Munichandraiah, *J. Phys. Chem. C* **2009**, *113*, 6303.
[47] F. Wang, S. Arai, M. Endo, *Carbon* **2005**, *43*, 1716.
[48] D. W. Wang, F. Li, M. Liu, G. Q. Lu, H. M. Cheng, *Angew. Chem., Int. Ed.* **2008**, *47*, 373.
[49] X. Yu, A. Manthiram, *Phys. Chem. Chem. Phys.* **2015**, *17*, 2127.
[50] R. Demir-Cakan, M. Morcrette, F. Nouar, C. Davoisne, T. Devic, D. Gonbeau, R. Dominko, C. Serre, G. Férey, J. M. Tarascon, *J. Am. Chem. Soc.* **2011**, *133*, 16154.